Particle Acceleration and Parallel Electric Field in Shock Waves

Hiromasa KAWAI, Seiichi TAKAHASHI, Yukiharu OHSAWA,
Shunsuke USAMI[1], Charles CHIU[2], and Wendell HORTON[2]

Department of Physics, Nagoya University, Nagoya 464-8602, Japan
[1]*National Institute for Fusion Science, Toki 509-5292, Japan*
[2]*Institute for Fusion Science, The University of Texas at Austin, Austin, TX 78712, USA*

The electric field parallel to the magnetic field, $E_\parallel$, in nonlinear magnetosonic waves is analytically studied. The theory shows that $E_\parallel$ can be strong. Then, with use of one-dimensional, fully kinetic, relativistic, electromagnetic, particle simulations and with test particle calculations, the effect of $E_\parallel$ on particle acceleration in shock waves is examined for three different mechanisms: incessant acceleration of relativistic ions, acceleration of trapped electrons, and positron acceleration along the magnetic field.

Keywords: parallel electric field, nonlinear magnetosonic wave, particle acceleration, relativistic ions, trapped electrons, positron acceleration

1. Introduction

In the ideal magnetohydrodynamics (MHD), the electric field parallel to the magnetic field is zero, and it was generally thought that the parallel electric field $E_\parallel$ is quite weak in MHD phenomena in high-temperature plasmas [1, 2]. Recently, however, it has been shown that the parallel electric field can be strong in nonlinear magnetosonic waves [3].

In this paper, we briefly review the theory for the parallel electric field and study the effect of parallel electric field on particle acceleration in shock waves, with particle simulations [4, 5] and test particle calculations.

In this method, we first obtain the electromagnetic fields of a shock wave from a particle simulation, and then, using these fields, we carry out test particle calculations to analyze the motions of relativistic ions, electrons, and positrons. The shock speed $v_{\rm sh}$ is taken to be close to $c\cos\theta$, where θ is the angle between the external magnetic field and wave normal. We are concerned with the case $v_{\rm sh} \sim c\cos\theta$ because it is known that strong particle acceleration takes place in this condition; i.e., 1) nonthermal energetic ions can be incessantly accelerated near the shock front owing to the relativistic effect that the particle momentum can increase indefinitely while the particle speed is bounded by the speed of light c [6], 2) some electrons are reflected near the end of the main pulse of a shock wave and then accelerated and trapped in the main pulse region [7], and 3) positrons can be accelerated along the magnetic field in the shock transition region [8]. (Positrons could be present around pulsars [9]-[12].) We compare the test particle motions calculated with two different methods; in the first method, the total electric field $\boldsymbol{E}$ is used in the relativistic equation of motion, while in the second method, $E_\parallel$ is omitted.

These studies confirm that in the acceleration of relativistic ions the parallel electric field becomes less important as the particle energy increases. For the acceleration of positrons and trapped electrons, however, $E_\parallel$ plays an essential role.

2. Overview of the Theory of Parallel Electric Field

The electric field parallel to the magnetic field was thought to be weak in MHD phenomena in high-temperature plasmas. In fact, from one of the basic equations of the ideal MHD,

$$\boldsymbol{E} + \frac{\boldsymbol{v} \times \boldsymbol{B}}{c} = 0, \tag{1}$$

one finds that the parallel electric field is zero,

$$E_\parallel = \frac{\boldsymbol{E} \cdot \boldsymbol{B}}{B} = 0. \tag{2}$$

The integral of $E_\parallel$ along the magnetic field,

$$F = -\int E_\parallel ds, \tag{3}$$

is thus also zero. The quantity F is referred to as the parallel pseudo potential in this paper.

In the two-fluid model, the parallel electric field in nonlinear magnetosonic waves is given as

$$E_\parallel = -\frac{\Gamma_e T_e}{e} \frac{\partial}{\partial s}\left(\frac{n_1}{n_0}\right), \tag{4}$$

where T_e is the electron temperature, Γ_e is the specific heat ratio, s is the length along the magnetic field, and n_0 and n_1 are the equilibrium and perturbed plasma densities, respectively [13]. One can obtain Eq.(4) with use of the conventional reductive perturbation method [14, 15]. Furthermore, by integrating Eq. (4), one finds the parallel pseudo potential as

$$eF = \Gamma_e T_e \frac{n_1}{n_0} \sim \epsilon \, \Gamma_e T_e, \tag{5}$$

where ϵ is the wave amplitude. The magnitude of F is determined by the electron temperature and is proportional to the wave amplitude.

Some particle simulations, however, show that eF far exceeds the electron temperature; for instance, the magnitude of eF shown in Ref. [7], which discussed the acceleration of electrons trapped by a shock wave, is roughly a half of the electric potential and is $\sim 10 m_e c^2$. The electron temperature alone cannot explain the large parallel pseudo potential observed in the particle simulations.

In order to see the effect of the magnetic field on $E_\parallel$, we consider the case in which the plasma temperature is zero ($T_e = T_i = 0$) and carry out higher order calculations with the reductive perturbation method, introducing the stretched coordinates:

$$\xi = \epsilon^{1/2}(x - v_A t), \tag{6}$$

$$\tau = \epsilon^{3/2} t, \tag{7}$$

where v_A is the Alfvén speed. In this cold plasma model, the parallel electric field and parallel pseudo potential are found to be

$$eE_\parallel = m_i v_A^2 \cos\theta \left(\frac{c}{\omega_{pe}}\right)^2 \frac{\partial^3}{\partial \xi^3} \frac{B_{z1}}{B_0}, \tag{8}$$

$$eF = -m_i v_A^2 \left(\frac{c}{\omega_{pe}}\right)^2 \frac{\partial^2}{\partial \xi^2} \frac{B_{z1}}{B_0} \sim \epsilon^2 m_i v_A^2. \tag{9}$$

Here, the waves are supposed to propagate in the x direction in an external magnetic field in the (x, z) plane, $\boldsymbol{B}_0 = B_0(\cos\theta, 0, \sin\theta)$. We have thus found that in small-amplitude pulses, the magnitude of the parallel pseudo potential is $eF \sim \epsilon \Gamma_e T_e$ in warm plasmas and is $eF \sim \epsilon^2 m_i v_A^2$ in cold plasmas.

Furthermore, for large-amplitude waves with $\epsilon \sim O(1)$ (shock waves), the relation

$$eF \sim \epsilon(m_i v_A^2 + \Gamma_e T_e), \tag{10}$$

explains the simulation results for both warm and cold plasmas [3]. This indicates that the parallel electric field can be quite strong in nonlinear magnetosonic waves.

3. Incessant Acceleration of Relativistic Ions

If the velocity v of an ion is so high that it exceeds the shock speed v_{sh} and the gyroradius of the particle is much greater than the width of the shock transition region, this particle can move back and forth between the shock wave and the upstream region in association with its gyromotion. This particle can gain energy from the transverse electric field when it is in the shock wave, because the gyromotion in the shock wave is nearly parallel to the transverse electric field in the shock wave. If the particle enters the shock wave at

$t = t_{in}$ and goes out to the upstream region at $t = t_{out}$, then the increment of its Lorentz factor γ in the period $t = t_{out} - t_{in}$ is given as

$$
\begin{aligned}
\delta\gamma &= \frac{2 q_i p_{1\perp} E_{1\perp}}{m_i^2 c^2 \Omega_{i1}} \sin\left(\frac{\Omega_{i1}(t_{out} - t_{in})}{2\gamma}\right) \\
&\quad + \frac{q_i}{m_i c^2} \int_{t_{in}}^{t_{out}} v_\parallel E_\parallel dt, \tag{11}
\end{aligned}
$$

where Ω_i is the nonrelativistic ion gyrofrequency; the subscript $\perp$ and 1, respectively, refer to vector components perpendicular to $\boldsymbol{B}$ and quantities in the shock wave [6]. Furthermore, if $v_{sh} \sim v_\parallel \cos\theta$, where $v_\parallel$ is the parallel velocity of the particle, this particle can move with the shock wave for a while. Because of the structure of the magnetic field in the shock transition region, the momentum parallel to the magnetic field, $p_\parallel$, increases when the particle enters and then goes out from the shock wave to the upstream region; i.e., $p_\parallel(t_{out}) - p_\parallel(t_{in}) > 0$. The parallel velocity therefore rises, and $v_\parallel \cos\theta$ becomes greater than the shock speed v_{sh}. As a result, the particle that was gyrating near the shock transition region therefore goes away from the shock wave to the upstream region, and the interaction with the shock wave ceases.

If the shock speed v_{sh} is close to $c \cos\theta$, however, some particles would move with the shock wave for long periods of time, much longer than their relativistic gyroperiods. Although the momentum can increase indefinitely, the velocity is bounded by the speed of light c. Because of this relativistic effect, particles cannot easily go faster than the shock wave if $v_{sh} \sim c \cos\theta$. Particles can move with the shock wave for long periods of time and repeatedly suffer energy jumps given by Eq. (11) in association with their gyromotion.

This acceleration mechanism has been studied with theory and particle simulations in Ref. [6]. In the theoretical analysis, the effect of the parallel electric field, such as the second term on the right-hand side of Eq. (11), was ignored, because the parallel electric field was thought to be weak in MHD phenomena in high-temperature plasmas.

We now quantitatively examine the effect of the parallel electric field with test particle calculations; that is, we carry out a shock simulation with one-dimensional (one space coordinate and three velocities), fully kinetic, fully electromagnetic particle code and then, by using the electric and magnetic fields obtained by the simulation, we follow test particle orbits. In the test particle calculations, we adopt two different methods. In the first method, we use the total electric field in the relativistic equation of motion,

$$\frac{d\boldsymbol{p}}{dt} = e\boldsymbol{E} + e\frac{\boldsymbol{v} \times \boldsymbol{B}}{c}, \tag{12}$$

while in the second method the parallel electric field
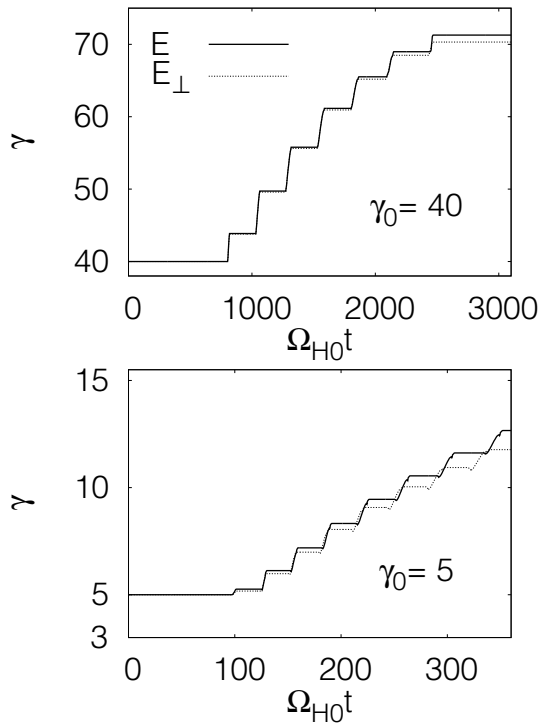
Fig. 1 Time variations of the Lorentz factors γ of test particles that are calculated with the total electric field (solid lines) and with the perpendicular electric field (dotted lines). The initial Lorentz factors are $\gamma_0 = 40$ in the upper panel and $\gamma_0 = 5$ in the lower panel. The difference between the solid and dotted lines is smaller in the higher energy case (upper panel) than in the lower energy case (lower panel).

is omitted in the equation of motion,

$$\frac{d\boldsymbol{p}}{dt} = e\boldsymbol{E}_\perp + e\frac{\boldsymbol{v} \times \boldsymbol{B}}{c}, \qquad (13)$$

where $\boldsymbol{E}_\perp$ is the perpendicular electric field. We then compare the motions obtained by these two methods.

The parameters of the particle simulation are as follows: The ion-to-electron mass ratio is $m_i/m_e = 400$; the speed of light is $c/(\omega_{pe}\Delta_g) = 10$, where Δ_g is the grid spacing; the external magnetic field is in the (x, z) plane with $\theta = 60°$ with its strength being $|\Omega_e|/\omega_{pe} = 3.1$. The Alfvén speed is thus $v_A/(\omega_{pe}\Delta_g) = 1.55$.

The test particles are initially put in the upstream region with the momentum distribution function

$$f(\boldsymbol{p}) = \frac{N}{4\pi p_0^2}\delta(p - p_0), \qquad (14)$$

where N is the number of test particles, and p_0 is related to the initial Lorentz factor through $\gamma_0 = [1 + p_0^2/(m_i^2 c^2)]^{1/2}$.

The upper panel of Fig. 1 shows the time variations of the Lorentz factors γ of relativistic test ions, in which the solid and dotted lines, respectively, represent the values calculated with use of the total electric

field $\boldsymbol{E}$ and with the perpendicular electric field $\boldsymbol{E}_\perp$. Their initial positions and velocities are the same, with $\gamma_0 = 40$. These particles suffer energy jumps seven times, and the two Lorentz factors exhibit quite similar behavior. Their difference $\gamma - \gamma_\perp$, where $\gamma_\perp$ is the Lorentz factor obtained from $\boldsymbol{E}_\perp$, is quite small; $(\gamma - \gamma_\perp)/\gamma = 1.4 \times 10^{-2}$ immediately after the seventh jump.

The lower panel of Fig. 1 shows the same figure for a lower energy case, $\gamma_0 = 5$. Even in this case, the two lines are quite close. Their difference, $(\gamma - \gamma_\perp)/\gamma = 5.9 \times 10^{-2}$, however, is slightly larger than that in the higher energy case.

These results indicate that the effect of the parallel electric field becomes small as the particle energy rises. The approximation ignoring $E_\parallel$ in the theoretical analysis of energetic-particle motions [6] is therefore valid.

4. Acceleration of Trapped Electrons

Some electrons are reflected in the end of the main pulse region (first large pulse) in an oblique shock wave. These particles are then trapped in the main pulse region and are accelerated to ultrarelativistic energies [7]. The energy of an accelerated electron is given as

$$m_e c^2 \gamma = \frac{e\phi}{1 - (v_{\rm sh}/c)(B_{z0}/B_{x0})}, \qquad (15)$$

in the wave frame, where ϕ is the electric potential. The Lorentz factor γ becomes especially large when $1 \sim (v_{\rm sh}/c)(B_{z0}/B_{x0})$; this relation can be written as $v_{\rm sh} \sim c\cos\theta$ in the laboratory frame. The electron reflection, which triggers the strong acceleration, occurs when the parallel pseudo potential F becomes small in the end of the main pulse region. The parallel electric field thus plays a crucial role in this acceleration mechanism.

To clearly see the effect of $E_\parallel$, we again perform the test particle calculations with use of the total electric field, Eq. (12), and with the perpendicular electric field, Eq. (13).

The top panel of Fig. 2 shows the phase space (x, γ) of electrons in the particle simulation, while the second and bottom panels show, respectively, the test electrons calculated with $\boldsymbol{E}$ and with $\boldsymbol{E}_\perp$. In the top and second panels, many electrons are trapped and have ultrarelativistic energies in the main pulse region of the shock wave. On the other hand, in the bottom panel, no electrons are trapped there. It is thus concluded that without the parallel electric field the electron reflection in the end of the main pulse and resultant particle acceleration does not occur.
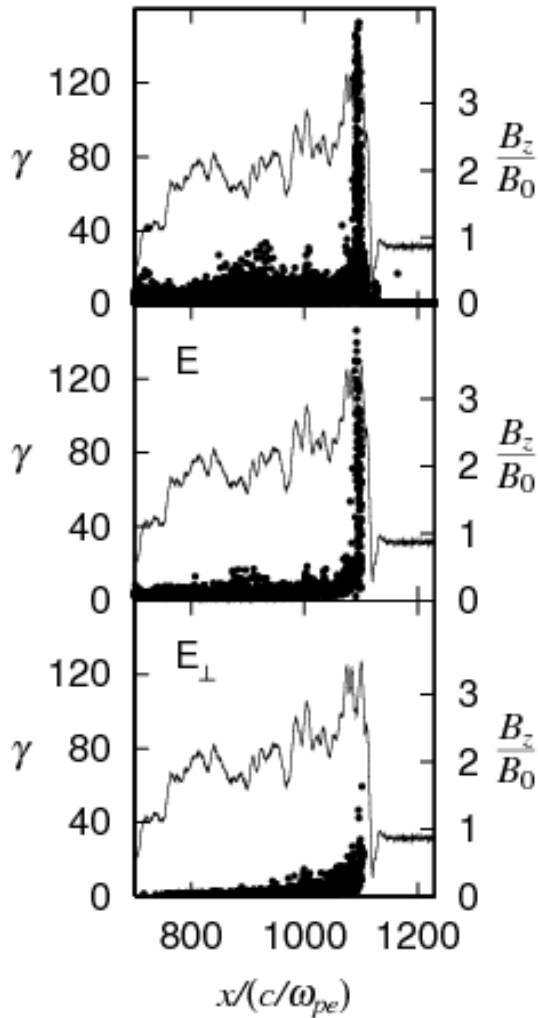
Fig. 2 Electron phase space plots (x, γ) and magnetic-field profiles (solid lines). The top panel shows the result of a particle simulation, while the second and bottom panels display test electrons calculated with $\boldsymbol{E}$ and with $\boldsymbol{E}_\perp$, respectively. The phase spaces of the top and second panels are quite similar, with many high-energy electrons near the shock front. In the bottom panel, there are few high-energy electrons.

5. Positron Acceleration along the Magnetic Field

In an electron-positron-ion plasma, oblique shock waves can accelerate positrons in the direction parallel to the magnetic field [8]. These positrons stay in the shock transition region and gain energy from the parallel electric field. Under the assumption that

$$\frac{d(\gamma \boldsymbol{v})}{dt} \simeq \boldsymbol{v}\frac{d\gamma}{dt}, \tag{16}$$

and $v_x \simeq v_{\rm sh}$, we obtain, after some algebra, the zeroth-order solution, in which v_y is small and $v_x/v_z = B_{x0}/B_{z0}$. The time rate of change of γ is given as

$$\frac{1}{\Omega_{p0}}\frac{d\gamma}{dt} = \frac{c\cos\theta}{v_{\rm sh}}\frac{(\boldsymbol{E}\cdot\boldsymbol{B})}{(\boldsymbol{B}\cdot\boldsymbol{B}_0)}, \tag{17}$$
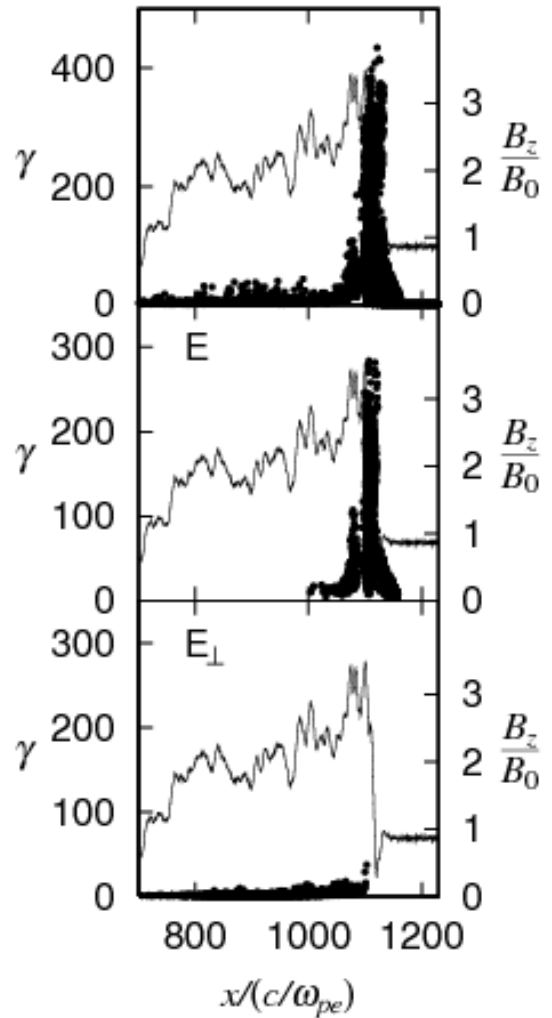
Fig. 3 Phase spaces of positrons in a particle simulation (top panel), test positrons calculated with $\boldsymbol{E}$, and test positrons calculated with $\boldsymbol{E}_\perp$. The bottom panel has no high-energy positrons.

where Ω_{p0} is the nonrelativistic positron gyrofrequency in the upstream region. The energy increase rate is proportional to the parallel electric field.

To examine the positron acceleration, we also carry out test particle calculations with use of Eq. (12) and with use of Eq. (13). Figure 3 shows the phase spaces of the positrons in a particle simulation (top panel), test positrons calculated with the total electric field (second panel), and test positrons calculated with the perpendicular electric field (bottom panel). The phase space plots of the top and second panels are quite similar, while in the bottom panel we find no high-energy positrons, indicating that in the absence of the parallel electric field the acceleration of positrons along the magnetic field does not occur.

6. Summary

We have described the parallel electric field in nonlinear magnetosonic waves and examined the effect

of $E_\parallel$ on particle acceleration. Specifically, we have investigated the three acceleration mechanisms: relativistic ions [6], trapped electrons [7], and positrons [8]. To do this, we first performed particle simulations for shock waves, and then, using the electric and magnetic fields obtained from the shock simulation, we followed the orbits of test particles. For the test particle calculations, we have adopted two methods; in the first method we have used the total electric field in the equation of motion while in the second method we have used the perpendicular electric field. The results of the two methods are compared. These studies confirm that the parallel electric field is unimportant in the acceleration of relativistic ions if their energies are sufficiently high. The reflection of electrons does not occur in the absence of $E_\parallel$; thus the trapping and acceleration of electrons does not occur either. Positron acceleration along the magnetic field is not observed without $E_\parallel$.

[1] H. Alfvén and C.-G. Fälthammer, *Cosmical Electro-dynamics*, (Clarendon Press, Oxford, 1963).

[2] J. V. Hollweg, Astrophys. J. **277**, 392 (1984).

[3] S. Takahashi and Y. Ohsawa, Phys. Plasmas **14**, 112305 (2007); S. Takahashi, M. Sato, and Y. Ohsawa, Phys. Plasmas **15**, 082309 (2008).

[4] A. B. Langdon and C. K. Birdsall, Phys. Fluids **13**, 2115 (1970).

[5] P. C. Liewer, A. T. Lin, J. M. Dawson, and M. Z. Caponi, Phys. Fluids **24**, 1364 (1981).

[6] S. Usami and Y. Ohsawa, Phys. Plasmas **9**, 1069 (2002); *ibid.* **11**, 3203 (2004).

[7] N. Bessho and Y. Ohsawa, Phys. Plasmas **6**, 3076 (1999); *ibid.* **9**, 979 (2002).

[8] H. Hasegawa, S. Usami, and Y. Ohsawa, Phys. Plasmas **10**, 3455 (2003); H. Hasegawa, K. Kato, and Y. Ohsawa, Phys. Plasmas **12**, 082306 (2005).

[9] P. A. Sturrock, Astrophys. J. **164**, 529 (1971).

[10] C. F. Kennel and R. Pellat, J. Plasma Phys. **15**, 335 (1976).

[11] J.-I. Sakai and T. Kawata, J. Phys. Soc. Jpn. **49**, 753 (1980).

[12] K. Hirotani, S. Iguchi, M. Kimura, and K. Wajima, Publ. Astron. Soc. Japan **51**, 263 (1999).

[13] Y. Ohsawa, Phys. Fluids **29**, 1844 (1986).

[14] T. Kakutani, H. Ono, T. Taniuti, and C. C. Wei, J. Phys. Soc. Jpn. **24**, 1159 (1968).

[15] T. Kakutani and H. Ono, J. Phys. Soc. Jpn. **26**, 1305 (1969).